Integration of multi-omic annotation data to prioritize and characterize inflammation and immune-related risk variants in squamous cell lung cancer

Ryan Sun[1], Miao Xu[2,3], Xihao Li[2], Sheila Gaynor[2], Hufeng Zhou[2], Zilin Li[2], Yohan Bossé[4], Stephen Lam[5], Ming-Sound Tsao[6], Adonina Tardon[7], Chu Chen[8], Jennifer Doherty[8,9], Gary Goodman[10], Stig Egil Bojesen[11,12,13], Maria Teresa Landi[14], Mattias Johansson[15], John K. Field[16], Heike Bickeböller[17], H-Erich Wichmann[18,19,20], Angela Risch[21,22,23], Gadi Rennert[24], Suzanne Arnold[25], Xifeng Wu[26], Olle Melander[27,28], Hans Brunnström[29], Loic Le Marchand[30], Geoffrey Liu[31], Angeline Andrew[9], Eric Duell[27], Lambertus A. Kiemeney[32], Hongbing Shen[33], Aage Haugen[34], Mikael Johansson[35], Kjell Grankvist[36], Neil Caporaso[14], Penella Woll[37], M. Dawn Teare[38], Ghislaine Scelo[15], Yun-Chul Hong[39], Jian-Min Yuan[40], Philip Lazarus[41], Matthew B. Schabath[42], Melinda C. Aldrich[43], Demetrios Albanes[44], Raymond Mak[45], David Barbie[46], Paul Brennan[15], Rayjean J. Hung[47], Christopher I. Amos[48], David C. Christiani[49,50], and Xihong Lin[2,51,*]

[1]Department of Biostatistics, University of Texas MD Anderson Cancer Center, Houston, Texas, United States of America

[2]Department of Biostatistics, Harvard T.H. Chan School of Public Health, Boston, Massachusetts, United States of America

[3]State Key Laboratory of Oncology in South China, Sun Yat-sen University Cancer Center, Guangzhou, China

[4]Institut Universitaire de Cardiologie et de Pneumologie de Quebec, Quebec, Canada

[5]British Columbia Cancer Agency, University of British Columbia, Vancouver, Canada

[6]Princess Margaret Cancer Centre, University Health Network, Toronto, Canada

[7]Faculty of Medicine, University of Oviedo and CIBERESP, Oviedo, Spain

[8]Department of Epidemiology, Fred Hutchinson Cancer Research Center, Seattle, Washington, United States of America

[9]Department of Epidemiology, Geisel School of Medicine, Hanover, New Hampshire, United States of America

[10]Department of Medical Oncology, Swedish Medical Group, Seattle, Washington, United States of America

[11]Copenhagen General Population Study, Herlev and Gentofte Hospital, Herlev, Denmark

[12]Department of Clinical Biochemistry, Herlev and Gentofte Hospital, Herlev, Denmark

[13]Faculty of Health and Medical Sciences, University of Copenhagen, Copenhagen, Denmark

[14]Division of Cancer Epidemiology and Genetics, National Cancer Institute, National Institutes of Health, Bethesda, Maryland, United States of America

[15]Genetic Epidemiology Group, International Agency for Research on Cancer, Lyon, France

[16]Institute of Translational Medicine, University of Liverpool, Liverpool, United Kingdom

[17]Department of Genetic Epidemiology, University Medical Center, Georg-August-University, Göttingen, Germany

[18]Institute of Medical Informatics, Biometry and Epidemiology, Ludwig Maximilians University, Munich, Germany

[19]Institute of Epidemiology, Helmholtz Center Munich, Neuherberg, Germany

[20]Institute of Medical Statistics and Epidemiology, Technical University Munich, Munich, Germany

[21]Cancer Cluster Salzburg, University of Salzburg, Salzburg, Austria

[22]Translational Lung Research Center Heidelberg, University Hospital Heidelberg, Heidelberg, Germany
[23]Translational Lung Research Center, German Center for Lung Research, Heidelberg, Germany
[24]Clalit National Cancer Control Center, Carmel Medical Center, Haifa, Israel
[25]Markey Cancer Center, University of Kentucky, Lexington, Kentucky, United States of America
[26]Department of Epidemiology, The University of Texas MD Anderson Cancer Center, Houston, Texas, United States of America
[27]Unit of Nutrition and Cancer, Catalan Institute of Oncology Barcelona, Spain
[28]Department of Clinical Sciences Malmö, Lund University, Lund, Sweden
[29]Laboratory Medicine Region, Skäne University Hospital, Lund, Sweden
[30]Epidemiology Program, University of Hawaii Cancer Center, Honolulu, Hawaii, United States of America
[31]Lunenfeld-Tanenbaum Research Institute, Sinai Health System, Toronto, Canada
[32]Faculty of Medical Sciences, Radboud University Medical Center, Nijmegen, The Netherlands
[33]Department of Epidemiology and Biostatistics, Nanjing Medical University, Nanjing, China
[34]National Institute of Occupational Health, Oslo, Norway
[35]Department of Radiation Sciences, Umeä University, Umeä, Sweden
[36]Department of Medical Biosciences, Umeä University, Umeä, Sweden
[37]Department of Oncology, University of Sheffield, Sheffield, United Kingdom
[38]School of Health and Related Research, University of Sheffield, Sheffield, United Kingdom
[39]Department of Preventive Medicine, Seoul National University College of Medicine, Seoul, Republic of Korea

[40]University of Pittsburgh Medical Center Hillman Cancer Center, University of Pittsburgh School of Medicine, Pittsburgh, Pennsylvania, United States of America

[41]Department of Pharmaceutical Sciences, Washington State University, Spokane, Washington, United States of America

[42]Department of Cancer Epidemiology, H. Lee Moffitt Cancer Center and Research Institute, Tampa, Florida, United States of America

[43]Department of Thoracic Surgery, Vanderbilt University Medical Center, Nashville, Tennessee, United States of America

[44]Russian N.N. Blokhin Cancer Research Centre, Russian Academy of Medical Sciences, Moscow, Russia

[45]Department of Radiation Oncology, Dana-Farber Cancer Institute, Boston, Massachusetts, United States of America

[46]Department of Medical Oncology, Dana-Farber Cancer Institute, Boston, Massachusetts, United States of America

[47]Prosserman Centre for Population Health Research, Sinai Health System, Toronto, Canada

[48]Dan L. Duncan Comprehensive Cancer Center and Department of Medicine, Baylor College of Medicine, Houston, Texas, United States of America

[49]Department of Environmental Health, Harvard T.H. Chan School of Public Health, Boston, Massachusetts, United States of America

[50]Department of Medicine, Massachusetts General Hospital, Harvard Medical School, Boston, Massachusetts, United States of America

[51]Department of Statistics, Harvard University, Cambridge, Massachusetts, United States of America

*Corresponding author

E-mail: xlin@hsph.harvard.edu

Funding: National Institutes of Health: R35-CA197449, R01-HL113338, P42-ES016454, U01CA209414, U19CA203654, and T32-ES007142. Christopher I. Amos is a research scholar of the Cancer Prevention Institute of Texas and is partially supported by RR170048.

Abstract

Clinical trial results have recently demonstrated that inhibiting inflammation by targeting the interleukin-1β pathway can offer a significant reduction in lung cancer incidence and mortality, highlighting a pressing and unmet need to understand the benefits of inflammation-focused lung cancer therapies at the genetic level. While numerous genome-wide association studies (GWAS) have explored the genetic etiology of lung cancer, there remains a large gap between the type of information that may be gleaned from an association study and the depth of understanding necessary to explain and drive translational findings. Thus, in this work we jointly model and integrate extensive multi-omics data sources, utilizing a total of 40 genome-wide functional annotations that augment previously published results from the International Lung Cancer Consortium (ILCCO) GWAS, to prioritize and characterize single nucleotide polymorphisms (SNPs) that increase risk of squamous cell lung cancer through the inflammatory and immune responses. Our work bridges the gap between correlative analysis and translational follow-up research, refining GWAS association measures in an interpretable and systematic manner. In particular, re-analysis of the ILCCO data highlights the impact of highly-associated SNPs from nuclear factor-κB signaling pathway genes as well as major histocompatibility complex mediated variation in immune responses. One consequence of prioritizing likely functional SNPs is the pruning of variants that might be selected for follow-up work by over an order of magnitude, from potentially tens of thousands to hundreds. The strategies we introduce provide informative and interpretable approaches for incorporating extensive genome-wide annotation data in analysis of genetic association studies.

Keywords: genome-wide annotation, integrative omics, lung cancer, major histocompatibility complex

Main Text

1 Introduction

Genome-wide association studies (GWAS) have successfully identified many genetic loci associated with lung cancer, however it is often difficult to explain exactly how associated variants perturb biological processes and increase risk of disease (Edwards, Beesley, French, & Dunning, 2013; Tam et al., 2019). Such difficulties arise in part from a conventional focus on only a few data types - for instance, genotype or gene expression data - which may naturally limit our understanding of the processes involved in carcinogenesis. Recently, many quantitative tools such as fine-mapping have been applied to better prioritize single nucleotide polymorphisms (SNPs) implicated in lung cancer (Ferreiro-Iglesias et al., 2018), but these approaches are also generally applied to only a few types of data. Less effort has been focused on cogently integrating the dozens of multi-omic annotations that offer a range of distinct perspectives regarding the mechanistic roles of individual SNPs (ENCODE Project Consortium, 2012; Visscher et al., 2017) associated with lung cancer.

This paper integrates forty different genome-wide variant functional annotations in a generalized linear mixed model (GLMM) based approach to prioritize and characterize inflammatory- and immune-related risk SNPs identified by a large-scale GWAS of lung squamous cell carcinoma (SCC) recently conducted by the International Lung Cancer Consortium (ILCCO) (McKay et al., 2017). Functional annotations describe characteristics of SNPs in a manner that parallels the way covariates describe subjects in a traditional GWAS regression analysis; one example of an annotation is the distance (in bp) between a SNP and the nearest transcription start site. The 40 annotations we use can thus be thought of as 40 covariates describing each SNP. In contrast to

147 association-based methods such as fine-mapping, our model utilizes genome-wide annotation
148 data from a variety of modalities to predict the biological roles of a SNP. The multi-dimensional
149 functional prediction recognizes that different types of variants can possess vastly different
150 consequences and thus allows SNPs to be evaluated on a range of attributes. This crucial feature
151 distinguishes the model from other aggregation algorithms, most of which produce a single
152 composite score that may be difficult to interpret and can over- or under-weight certain traits
153 based on factors such as the type of training data used (Huang, Gulko, & Siepel, 2017; Kircher et
154 al., 2014; Rogers et al., 2018).
155
156 Our re-analysis of the previously published ILCCO GWAS data – which reported a table of over
157 21,000 highly-associated (i.e. $p<10^{-5}$) SNPs - emphasizes the inflammatory response and related
158 immune mechanisms, which have long been studied as risk factors for lung cancer (Takahashi,
159 Ogata, Nishigaki, Broide, & Karin, 2010; Walser et al., 2008). We take this approach because of
160 a pressing and unmet need to more clearly explain significant results from the recent CANTOS
161 clinical trial. In this trial (P. M. Ridker et al., 2017), patients treated with 300 mg of
162 canakinumab, an IL-1β inhibitor, demonstrated a large decrease in lung cancer incidence (hazard
163 ratio=0.33, $p<0.0001$) and mortality (hazard ratio=0.23, $p=0.0002$) during median follow-up of
164 3.7 years, one of the first such successes when targeting IL-1β in randomized human trials for
165 lung cancer. CANTOS was primarily designed to evaluate cardiovascular outcomes and also
166 demonstrated a significant reduction in risk of recurrent cardiovascular events (Paul M Ridker et
167 al., 2017). It is of great interest to understand the genetic underpinnings of inflammatory- and
168 immune-based risk in SCC to, for example, provide a more direct view into the biological
169 mechanisms underlying disease, suggest possible therapeutic targets, or guide more accurate risk

screening policies, all goals difficult to achieve through association studies alone (Karczewski & Snyder, 2018). The main objective of our manuscript is to move toward these goals by identifying and characterizing translationally relevant SNPs that can be prioritized for functional follow-up studies. Accomplishing this objective can conserve many resources that would be needed to validate the tens of thousands of variants identified through GWAS alone, as prioritization can allow researchers to focus on a subset of GWAS variants that are likely to possess functional roles.

This synthesis of the multi-faceted variant functional annotation data highlights the roles of many SNPs in genes belonging to intricate regulatory networks that affect cytokine signaling cascades and the immune response. For example, we prioritize a number of regulatory SNPs in nuclear factor-κB (NF-κB) signaling pathway genes. We also uncover a number of variants in the HLA region that may perturb disease risk through disruption of standard antigen presenting processes. Comparisons with risk variants in other lung cancer subtypes suggest that the sets of genetic variants driving inflammation risk in these diseases differ from those highlighted in our analysis of SCC. Taken together, our results help explain the CANTOS findings at a genetic level, advance understanding of the inflammation and immune related systems driving lung cancer risk across different histologies, and demonstrate how to integrate varied sources of multi-omic variant annotation data in a coherent statistical framework.

2 Materials and Methods

2.1 Multi-dimensional annotation class estimation

To interrogate the mechanistic roles of individual variants, we utilized a Multi-dimensional Annotation Class Integrative Estimator (MACIE) (Li, 2020; Yung, 2016) that modeled a SNP's annotation values using a generalized linear mixed model in which the annotation values were assumed to depend on a SNP's membership in multiple latent binary classes. In the MACIE framework, function was defined as a composite of these unobserved classes, with each class designed to summarize the functionality described by a different set of annotations. This distinctive formulation of functionality as a set of multiple characteristics allowed for a more versatile and more interpretable model than was possible when considering only a single holistic score. Existing integrative methods that produce one-dimensional ratings often either sacrifice data to focus on a single attribute or sacrifice specificity to incorporate more annotations (Supplementary Figure S1).

The model-fitting procedure estimated latent variant functional classes in the GLMM setting, while accounting for correlations between multiple annotations using random effects, under previously specified models for this framework (Sammel, Ryan, & Legler, 1997). Estimation proceeded with the EM algorithm, and computation of MACIE occurred in two main stages. In the training stage, the MACIE model was constructed using functional scores (36 for noncoding and synonymous variants and 12 for nonsynonymous coding variants) from a properly selected training dataset. This step obtained the fitted model parameters. In the prediction stage, the fitted model parameters were applied to a new set of SNPs to calculate the probability that each SNP belonged to a specific functional category given the data (see Appendix A for technical details). The functionality of a noncoding or synonymous coding SNP was defined with a regulatory class and an evolutionarily conserved function class. The membership of a SNP in each class was

denoted by a binary indicator, and as such, the MACIE score was a composite measure corresponding to the probability that a SNP belonged to each of the $2 \times 2 = 4$ possible classes. Marginal probabilities for either the regulatory or conserved classes could also be calculated by summing the two probabilities corresponding to that class.

Functional annotation scores were selected and partitioned into three groups (regulatory function, evolutionarily conserved function, damaging protein function) based on previous experience (Yung, 2016) with modeling the annotations most likely to add novel and useful information in predicting functional roles. Different scores and different partitions could additionally be used for different phenotypes; such a step would require the model to be retrained. All precomputed scores for the specific MACIE model used in this analysis are available online (see Data Availability Statement).

All 40 scores used in the model were downloaded from the EIGEN (Ionita-Laza, McCallum, Xu, & Buxbaum, 2016) and CADD (Kircher et al., 2014) databases. Missing values were imputed as described in the original databases. As with EIGEN (Ionita-Laza et al., 2016), we retrieved each variant's functional class from the CADD database and grouped "Regulatory", "Intronic", "Downstream", "Upstream", "Noncoding change", "3prime UTR", "5prime UTR", "Intergenic", and "Synonymous" SNPs all in the same noncoding and synonymous variants group. The MACIE training dataset for these variants consisted of 10% of variants randomly selected from the 1000 Genomes Project data set (excluding those in dbNSFP) that were located within 500 bp upstream of a gene start site.

For each variant, the conserved class integrated eight evolutionary conservation scores downloaded from the EIGEN database: GERP_NR, GERP_RS, PhyloPri, PhyloPla, PhyloVer, PhastPri, PhastPla, and PhastVer (names given as they appear in EIGEN). These scores corresponded to outputs from the GERP++, phyloP, and phastCons algorithms and were previously described (Davydov et al., 2010; Ionita-Laza et al., 2016; Pollard, Hubisz, Rosenbloom, & Siepel, 2010; Siepel et al., 2005). The transcription regulatory class integrated 28 functional scores from the CADD database (Kircher et al., 2014), including GC, CpG, ENCODE histone modification marks (EncH3K27Ac, EncH3K4Me1, EncH3K4Me3), ENCODE open chromatin marks (EncExp, EncOCCombPVal, EncOCDNasePVal, EncOCFairePVal, EncOCpolIIPVal, EncOCctcfPVal, EncOCmycPVal, EncOCDNaseSig, EncOCFaireSig, EncOCpolIISig, EncOCctcfSig, EncOCmycSig), ENCODE transcription factor binding sites data (TFBS, TFBSPeaks, TFBSPeaksMax), ChromHMM states collapsed into 5 groups (cHmmTSS, cHmmTx, cHmmEnh, cHmmZnf, cHmmRepr), bStatistic, minDistTSS, and minDistTSE (all names as they appear in the CADD database). The MACIE GLMM for noncoding and synonymous SNPs was then fit by jointly integrating all 36 functional scores in two classes.

For the nonsynonymous model, the training set used 10% of variants in the dbNSFP database (Liu, Wu, Li, & Boerwinkle, 2016), excluding sex chromosomes. The same eight conservation scores as above were used to evaluate an evolutionarily conserved class, and then four protein function scores (SIFT (Ng & Henikoff, 2003), PolyPhenDiv (Adzhubei et al., 2010), PolyPhenVar, and Mutation Assessor (Reva, Antipin, & Sander, 2011)) were extracted from the EIGEN database and used to predict a second class assessing the damaging function of coding

substitutions. The MACIE marginal probabilities were then calculated using the same procedures described for noncoding variants.

2.2 Gene-based association analysis

To focus the analysis on inflammatory- and immune-related processes, we first performed gene-level inference on the largest existing lung cancer GWAS dataset. While MACIE results were calculated for all ILCCO SNPs, a key feature of the model was interpretability of the predicted classes, and so to most clearly demonstrate this advantage we concentrated discussion on those SNPs located near inflammatory- and immune-related genes. SNPs that were not located near genes but still predicted to belong to MACIE functional classes were interesting in their own right, although we left their exploration for future work.

Collection and preparation of the complete ILCCO OncoArray dataset was described previously (McKay et al., 2017), and from this overall compendium we restricted our initial gene-based association analysis to a subset of 7,426 squamous cell carcinoma cases and 55,630 controls, all of European descent. We mapped (Aken et al., 2016; Chang et al., 2015) individual SNP test statistics to genes if they fell inside or within 5 kb of the gene.

Gene-based inference was conducted with the Generalized Berk-Jones (GBJ) statistic (Sun & Lin, 2019). GBJ was derived from the Berk-Jones statistic, which demonstrates certain asymptotic optimality properties in set-based testing situations, and GBJ was previously shown to provide more power than comparable methods such as the Sequence Kernel Association Test (Wu et al., 2011) over a variety of commonly-occurring testing situations.

All summary statistics used were derived from SNPs with a minor allele frequency greater than 1% in the 1000 Genomes European cohort, thus the normality assumption of GBJ was likely to be satisfied, given the very large sample size. For very large genes comprising more than 1,000 SNPs, we pruned the set to remove SNPs that were correlated at $r^2>0.5$ (Chang et al., 2015). Each different histology was tested with the ILCCO summary statistics corresponding to that histology.

In searching for functional SNPs conferring risk of SCC, we also limited our main analysis to variants possessing a marginal association of $p<5 \times 10^{-6}$ or uncommon and rare variants (minor allele frequency less than 5%) demonstrating $p<5 \times 10^{-4}$. The common threshold of 5×10^{-8} used for genome-wide significance was not employed both because this was not a hypothesis testing study and because highly functional SNPs may demonstrate only modest association due to the limitations of marginal models. A less stringent measure was used for uncommon and rare variants because they are widely believed to demonstrate more functionality.

2.3 Fine-mapping of HLA

Many variants in the HLA region showed both highly significant p-values and high MACIE predictions, and the density of strongly associated SNPs was much larger compared to other portions of the genome. Thus, we first performed additional imputation and fine-mapping to discover independent association signals amidst the strong long-range LD of this region. The original genotypes were imputed using 1000 Genomes Project data (1000 Genomes Project Consortium, 2015), but larger and richer datasets have been made available since then. We

utilized the SNP2HLA (Jia et al., 2013) software to reimpute data from the original OncoArray chip with a reference dataset from the Type I Diabetes Genetics Consortium (Rich & Concannon, 2015). We then followed previous lung cancer association studies (Ferreiro-Iglesias et al., 2018) by taking a forward stepwise regression approach with all original ILCCO SNPs as well as newly imputed SNPs to help determine the strongest independent signals in the highly polymorphic region.

3 Results

3.1 SCC-associated genes

Gene-based inference uncovered 243 genes (Supplementary Table S1) significantly associated with lung cancer risk at the Bonferroni-corrected level of $p=1.96 \times 10^{-6}$ (Figure 1a-c), with a number of the most highly associated genes mapping to regions of the genome that were validated in previous lung cancer studies (*IREB2, CHRNA5*, *ADAMTS7,* and others) (Bosse & Amos, 2018; Timofeeva et al., 2012). Of the 243 significant genes, 187 (77%) fell inside or within 2 Mb of the HLA complex (Supplementary Figure S2). Notably, many significant genes comprised important components of NF-κB signaling pathways. Examples included *TNF, CHUK, NFKBIL1,* and *TRIM38.* Multiple major histocompatibility complex (MHC) class I and class II genes were implicated as well, including *HLA-A, HLA-DQA1,* and *HLA-DQB1.* These inflammation and immune-related loci guided our search for functional variants.

3.2 Model-highlighted variants

In total, we found 868 SNPs meeting the marginal association threshold (see Materials and Methods) that were predicted to belong to the regulatory class with probability greater than 0.9

(Figure 1d), and we found 65 SNPs meeting the marginal association threshold that were predicted to belong to the evolutionarily conserved class with probability greater than 0.9 (Figure 1e). While some SNPs highlighted by the model possessed extremely significant p-values, the range of marginal association was also quite large (Supplementary Table S2-S5). SNPs with MACIE predictions close to one generally possessed many elevated functional scores (Figure 2-3), while variants with low predictions were often characterized by less remarkable annotation values. In the following, we highlight some of the strongest model predictions to show how results can supplement previous literature and existing work in a novel and efficient manner.

3.3 Variants near genes involved in NF-κB signaling

The NF-κB family possesses a number of different roles in the immune response and other biological processes (Zhang, Lenardo, & Baltimore, 2017), and regulation of NF-κB has been implicated in a wide variety of inflammation-based diseases, including many cancers (Hoesel & Schmid, 2013; Lawrence, 2009; Pikarsky et al., 2004). In their inactive state, NF-κB proteins are bound to the inhibitors of NF-κB (IκB) family (Dolcet, Llobet, Pallares, & Matias-Guiu, 2005). Activation can occur through the IκB kinase (IKK) complex (Karin & Greten, 2005).

TNF superfamily activation is an inducer of NF-κB signaling (Aggarwal, 2003) and is also one of the pathways that can be blocked by canakinumab-induced inhibition of IL-1β (Taniguchi & Karin, 2018). Members of the family including *TNF*, *LTA,* and *LTB* were three neighboring genes highly associated with SCC (all with gene-level $p<1 \times 10^{-12}$ for association with SCC), highlighting a link that has been observed in other inflammatory phenotypes as well (Dretzke et al., 2011; Van Schouwenburg, Rispens, & Wolbink, 2013). Two of the most significant SNPs in

353 the region were rs1800629 and rs1800628, found less than 1 kb upstream and downstream of the
354 *TNF* transcription start and end sites, respectively.
355
356 Based on data from 28 different measures of epigenetic activity, the regulatory class prediction
357 for rs1800629 was greater than 99% (Table 1). This estimate was driven by many elevated
358 annotation scores including, for example, ENCODE experiments demonstrating evidence of
359 open chromatin (Figure 2f). The variant rs1800629 was previously cataloged in curated sources
360 such as ClinVar (Landrum et al., 2014), has been referred to in the literature as TNF-308A, and
361 has seen its adenine substitution repeatedly associated with increased expression of *TNF*
362 (Karimi, Goldie, Cruickshank, Moses, & Abraham, 2009; Mira et al., 1999). Consistent with the
363 CANTOS hypothesis that inflammation contributes to lung cancer risk, the adenine minor allele
364 was risk-conferring for SCC (OR=1.16, $p=1.66 \times 10^{-8}$), indicating the possibility that
365 rs1800629 was linked with SCC because it increased *TNF* expression and thus also inflammatory
366 activity.
367
368 Although rs1800628 (OR=1.28, $p=1.54 \times 10^{-15}$) demonstrated a level of marginal association
369 that was multiple orders of magnitude more significant than its upstream counterpart rs1800629,
370 the MACIE prediction was less than 0.01 for both classes (Table 1) due to a lack of regulatory
371 and evolutionary conservation evidence (Figure 2-3) among the available data. The disparity in
372 p-values was possibly due to the limitations of marginal regressions, for example, rs1800628
373 may have fallen in strong linkage disequilibrium with another important SNP. rs1800628 may
374 also simply have possessed roles that were not probed by the existing classes as defined in the
375 model.

As a subunit of the IKK complex, *CHUK* (gene-level p=1.60×10^{-6} for association with SCC) was another key member of the NF-κB signaling cascade (Hacker & Karin, 2006) determined to be significantly associated with lung cancer risk. Although no SNPs in *CHUK* reached the standard genome-wide significance level of 5×10^{-8}, the combination of 26 SNPs with p-values less than 5×10^{-6} pushed the gene-level association between *CHUK* and SCC to significance. Integrated annotation analysis (Supplementary Figure S3) suggested the signal originated in part from rs28372851 (OR=1.25, p=5.18×10^{-7}), a variant located approximately 2 kb upstream of the transcription start site. This SNP was previously predicted (Fishilevich et al., 2017) to lie in an enhancer region of *CHUK,* and the combined data strongly estimated that rs28372851 belonged to the regulatory class, with a prediction score greater than 0.99 (probability conserved class less than 0.1%). The MACIE regulatory prediction was driven by multiple epigenetic features including high histone modification signal peaks (Supplementary Figure S3b-c). Increased expression of *CHUK* can further activate NF-κB (Hacker & Karin, 2006).

3.4 Variants near inhibitors of NF-κB signaling

The CANTOS trial illustrated that an IL-1β inhibitor could provide significant therapeutic benefits in lung cancer, so it followed that searching for genetic variation mimicking the function of canakinumab might also uncover SNPs with key protective roles. One such example was identified in *TRIM38* (gene-level p=1.26×10^{-12}), which was previously observed to inhibit cytokines, including TNF and IL-1β, that activate NF-κB (Hu & Shu, 2017). *TRIM38* reached gene-level significance in association with SCC due in part to 15 genome-wide significant SNPs, although many of them fell in high LD (Supplementary Figure S4a). In particular, the SNP

399 rs72832596 (OR=1.21, p=2.02×10^{-9}) possessed many elevated annotation values
400 (Supplementary Figure S4b-c) that contributed to a model prediction of greater than 0.99 for
401 inclusion in the class of regulatory SNPs (probability conserved class less than 0.1%,
402 Supplementary Figure S4d-e). Further validation was provided by the GTEx (GTEx Consortium
403 et al., 2013) project, which showed rs72832596 to be an eQTL of *TRIM38* in whole blood, as the
404 minor allele was associated with decreased expression of *TRIM38*. While GTEx discoveries
405 suffer from the same drawbacks as other association results, rely on small sample sizes, and are
406 not available for all SNPs with annotation data, positive eQTL findings do offer some evidence
407 of regulatory function. The minor allele also showed an effect direction (Supplementary Figure
408 S4f) consistent with a positive correlation between inflammation and disease risk. As immune
409 cells may comprise a significant proportion of whole blood, the expression-increasing allele at
410 rs72832596 could possibly be interpreted as a pseudo-dose of canakinumab increasing the level
411 of cytokine inhibition, thus reducing the amount of signaling by IL-1β and associated proteins
412 and leading to a decrease in inflammation.
413
414 A final highly significant gene in SCC with connections to cytokine regulatory networks was
415 *NFKBIL1* (gene-level p=3.04×10^{-12}), which has been shown to demonstrate IκB-like
416 functions (Chiba, Matsuzaka, et al., 2011; Hayden & Ghosh, 2012) and has been linked with,
417 among other inflammation-related phenotypes, rheumatoid arthritis (Chiba, Miyashita, et al.,
418 2011; Okamoto et al., 2003). The integrated annotation data highlighted rs2239527 (OR=1.10,
419 p=2.02×10^{-6}), a variant approximately 5 kb upstream (Supplementary Figure S5a) of
420 *NFKBIL1* that showed exceptional conservation across primates, mammals, and vertebrates with,
421 for example, large phastCons, phyloP, and GERP++ scores. These scores and others led the

model to predict that rs2239527 belonged to both the regulatory and conserved classes with probability approaching 1 (Supplementary Figure S5b-c). Results from multiple other alternative variant scoring systems also highlighted this variant (Supplementary Figure S5d-f).

3.5 HLA risk variants

Although the CANTOS trial demonstrated the therapeutic benefit of targeting cytokine signaling processes, annotation data also implicated other features of inflammatory and immune responses in conferring lung cancer risk. In particular, we previously noted that many of the most significant SNPs and genes associated with SCC fell in the HLA region. More specifically, variants in HLA genes prioritized by the MACIE model (Figure 4a-b) demonstrated a variety of links to the dysregulated immune response that has been observed in lung cancers (Carbone, Gandara, Antonia, Zielinski, & Paz-Ares, 2015; Gandhi et al., 2018; Palucka & Banchereau, 2012).

Re-imputation and fine-mapping in the HLA selected two independent association signals amidst the strong long-range LD of the HLA (Supplementary Table S6). The association and prediction models converged for *HLA-DQB1* variant rs1049133 (unconditional OR=1.18, $p=3.45 \times 10^{-8}$), which ranked as the second strongest independent association signal in the entire HLA and was predicted by the available annotation data to belong to the conserved class with probability 93.4%. *HLA-DQB1* (gene-level $p=4.10 \times 10^{-10}$) was significantly associated with SCC risk, and the protein is a receptor found on antigen-presenting cells. In contrast, the most significant SNP in the reimputation, rs3094604, did not show an annotation profile indicating that it belonged to one of the model classes (Table 1). Thus, this example again succinctly demonstrated the added

information generated by modeling annotation data. *HLA-DQB1* was also notable for its status as the gene with the second largest number of SNPs both passing the marginal association threshold and possessing a MACIE regulatory prediction of greater than 0.9, with 35 such SNPs. *HLA-DQA1* (gene-level $p<1 \times 10^{-12}$) held the most such SNPs with 86, and no other MHC-region gene held more than 11.

Additionally, many of the model-prioritized SNPs located outside *HLA-DQB1* and *HLA-DQA1* still showed strong links to these genes. Across all chromosomes there were only 868 SNPs passing the marginal association threshold and possessing a MACIE regulatory prediction of greater than 0.9, with 613 (71%) falling in the HLA region. Of these 613, 21% were eQTLs of *HLA-DQA1* in one or both of blood or lung tissue according to GTEx, and 29% were eQTLs of *HLA-DQB1* in one or both of blood or lung tissue according to GTEx (Supplementary Table S7), for a total of 562 eQTL findings across both tissues. Of the 562 SNP-expression pairs, over 99% of the effect directions were oriented such that the expression-lowering allele corresponded to the same allele associated with a marginal increase in SCC risk. The abundance of highly associated and model-prioritized SNPs that were previously validated as HLA eQTLs in blood and lung tissue suggested that many SNPs may contribute to SCC risk by modulating expression of MHC genes.

Many of the significantly associated SNPs in the HLA region were nonsynonymous coding SNPs, and for these variants we calculated a damaging protein substitution class instead of the regulatory class (see Materials and Methods). In general, highly linked nonsynonymous variants tended to demonstrate more variation in conservation class predictions. For example, in *HLA-*

DQA1 the missense variants rs707949 (OR=1.17, p=1.61×10^{-10}) and rs707962 (OR=1.18, p=1.23×10^{-10}), demonstrated correlation falling just below 1. However (Figure 4c-f), rs707949 earned a higher evolutionarily conserved class prediction of 0.85 compared to 0.12 for rs707962. As with all previous predictions, results should be interpreted with caution as some functionality of nonsynonymous SNPs – for example, their potential to influence the folding of *HLA-DQA1* - are roles not directly covered by existing classes in the MACIE model and demonstrate the potential for MACIE modeling of additional attributes once more annotations are available to predict other categories.

3.6 Significantly associated genes in other histologies

Previous reports have described the genetic bases of different lung cancer histologies as highly dissimilar (Wang et al., 2015); thus, important variants may differ and therapeutic strategies such as those used in CANTOS may see efficacy vary by subtype. To investigate whether the variants highlighted above may also contribute to risk of other lung cancer subtypes, we reperformed the initial step of our investigation by conducting separate gene-level analyses with the ILCCO adenocarcinoma and small cell lung cancer cases. Consistent with previous reports, we found that the top genes associated with SCC showed little overlap with the other two histologies. Compared to the 243 genes significant at the Bonferroni-corrected significance level in SCC, only 39 genes reached significance in adenocarcinoma (Fig 1b), even with a larger number of adenocarcinoma cases (11,270 compared to 7,426 for SCC). In particular, the inflammation-related genes *TNF, CHUK*, *TRIM38*, and *NFKBIL1* did not rank among the top 2,000 most significant genes, and no HLA genes passed the Bonferroni-corrected significance level. This difference could partly be attributable to the increased mutation burden associated with

squamous cell carcinoma of the lung. Small cell lung cancer showed even fewer significant genes (Figure 1c) with only 12 passing the Bonferroni threshold, although this low number was likely also impacted by the reduced sample size of 2,170 small cell lung cancer cases. Marginal association strength for previously mentioned SNPs also varied across histology (Supplementary Table S8).

As we previously detailed, association results are limited in scope and interpretation. However, by demonstrating the differences in significant genes between SCC and other histologies, we showed that a similar integrated analysis of adenocarcinoma or small cell lung cancer would likely identify many distinct variants.

4 Discussion

Genetic studies of lung cancer have often focused on extracting information from association analyses using only a few types of data. Yet, for such studies to further disentangle the disease's complex genetic etiology and provide more translational value, it is becoming increasingly important to integrate and utilize the full scope of available omics information, recorded from a wide range of experimental modalities (Freedman et al., 2011; Karczewski & Snyder, 2018). We attempted to advance this objective and refine results from the recent CANTOS clinical trial by harnessing a variety of diverse genomic datasets to elucidate how genetic variants identified through GWAS may confer lung SCC risk through inflammation and immune networks.

Our analysis identified hundreds of SNPs that demonstrate evidence of association with SCC and possessed a greater than 90% chance of inclusion in at least one of three classes: regulatory,

514 evolutionarily conserved, and protein damaging. These variants represented a filtration of the
515 tens of thousands of highly associated SNPs documented in the largest existing lung cancer
516 GWAS, which, for example, reported a table of over 21,000 highly associated SNPs. Our results
517 demonstrated that the most significant variants at GWAS risk loci may not necessarily be
518 functional SNPs (Supplementary Table 9), and hence it may not be desirable to simply select the
519 most significant variants for follow-up studies. By leveraging functional annotation information,
520 we showed that it is possible to select a much smaller subset of significantly associated SNPs for
521 follow-up. Such work can reduce the number of variants prioritized for additional studies by over
522 an order of magnitude and can translate to large cost and effort savings. In addition, our work
523 markedly contributed to knowledge about the functional mechanisms at each identified risk
524 locus, providing further quantitative and qualitative insight about how individual variants possess
525 roles in the major biological themes leading to lung cancer risk. We next summarize some of
526 these broader findings regarding risk factors for lung cancer.
527
528 In further analyzing SNPs selected by the integrative annotation analysis, we found indications
529 that the NF-κB inflammation signaling pathway and HLA-mediated immune responses were key
530 mechanisms in SCC disease progression. Specifically, multi-omics data from dozens of diverse
531 sources demonstrated that a number of annotation-prioritized SNPs were located near genes
532 involved in regulation of NF-κB activation and antigen presentation. Although our study is not
533 the first to link lung cancer with inflammation, NF-κB (Ben-Neriah & Karin, 2011; Taniguchi &
534 Karin, 2018), or the HLA region (Ferreiro-Iglesias et al., 2018), to our knowledge, it is among
535 the first attempts to integrate genome-wide functional annotation data with large-scale lung

cancer GWAS findings in pinpointing relevant variants and explaining the specific roles of these substitutions.

The abundance of variants highlighted in this report reinforces the view that lung cancer boasts a highly complex genetic etiology, with large networks of SNPs possessing non-trivial amounts of important behavior. Thus, as a complement to the traditional GWAS individual SNP association analysis, the novel approach outlined in this paper – identifying significant genes through set-based inference and leveraging rich external annotation data to assess the roles of significant SNPs in these genes – could likely be applied to search for genetic determinants of lung cancer risk in other biological systems as well. We emphasize that MACIE offers an unsupervised and highly interpretable tool allowing researchers to move beyond the conventional search for associations and instead determine the biological consequences of genetic variation. When applying the method to different traits, researchers should leverage disease-specific biological knowledge and should ensure that the classes and functional annotations used are relevant for the outcome of interest.

Our manuscript focused on squamous cell carcinoma because the vast majority of ILCCO SCC cases identified as current or past smokers; these subjects likely demonstrated a larger mutation burden and increased pulmonary inflammation due to tobacco smoke (Spitz et al., 2011), and therefore we expected inflammatory mechanisms to display a more direct connection with SCC than other lung cancer subtypes. Comparisons of SCC GWAS results with adenocarcinoma and small cell lung cancer revealed largely disparate profiles of genetically-induced inflammation risk. Hence our findings illustrated the importance of studying disease subtypes and considering

559 differing underlying biological mechanisms when utilizing IL-1β inhibitors as a strategy for
560 treating or preventing lung cancer.
561
562 The specific findings discussed in this manuscript offer many avenues for follow-up research.
563 The profusion of functional SNPs indicates that more precise interventions tailored to each
564 patient's individual genome may be more successful than wide-ranging therapies aimed at the
565 general population. Integrative investigations of other processes critical to lung cancer
566 progression will be essential as well. Further experimental validation will also be necessary to
567 continue refining the performance of data-driven predictions and provide additional evidence
568 linking specific variants to disease.
569
570 **Acknowledgements**
571 We thank the International Lung Cancer Consortium for use of their data and Dr. Song Gao of
572 Sun Yat-sen University Cancer Center for helpful conversations. We would also like to thank the
573 reviewers for their helpful comments that greatly improved the paper.
574
575 **Data Availability Statement**
576 Portions of the data used in this study were generated by the International Lung Cancer
577 Consortium and are available at the database of Genotypes and Phenotypes (dbGaP) under
578 accession phs001273.v1.p1 and phs000876.v1.p1. This is the same data that was published in
579 McKay et al., 2017. Additional ILCCO data is available upon request from
580 https://oncoarray.dartmouth.edu. The data are not publicly available due to privacy restrictions.
581 Annotation data was downloaded as described in Methods. All MACIE code, scores, and

582 annotation data used in this paper are available at

583 www.github.com/ryanrsun/lungCancerMACIE.

584 **References**

585 1000 Genomes Project Consortium. (2015). A global reference for human genetic variation.
586 *Nature, 526*(7571), 68-74. doi:10.1038/nature15393
587 Adzhubei, I. A., Schmidt, S., Peshkin, L., Ramensky, V. E., Gerasimova, A., Bork, P., . . .
588 Sunyaev, S. R. (2010). A method and server for predicting damaging missense mutations.
589 *Nature Methods, 7*(4), 248-249. doi:10.1038/nmeth0410-248
590 Aggarwal, B. B. (2003). Signalling pathways of the TNF superfamily: a double-edged sword.
591 *Nature Reviews: Immunology, 3*(9), 745-756. doi:10.1038/nri1184
592 Aken, B. L., Ayling, S., Barrell, D., Clarke, L., Curwen, V., Fairley, S., . . . Searle, S. M. (2016).
593 The Ensembl gene annotation system. *Database (Oxford), 2016*.
594 doi:10.1093/database/baw093
595 Ben-Neriah, Y., & Karin, M. (2011). Inflammation meets cancer, with NF-kappaB as the
596 matchmaker. *Nature Immunology, 12*(8), 715-723. doi:10.1038/ni.2060
597 Bosse, Y., & Amos, C. I. (2018). A decade of GWAS results in lung cancer. *Cancer*
598 *Epidemiology, Biomarkers & Prevention, 27*(4), 363-379. doi:10.1158/1055-9965.Epi-
599 16-0794
600 Carbone, D. P., Gandara, D. R., Antonia, S. J., Zielinski, C., & Paz-Ares, L. (2015). Non–small-
601 cell lung cancer: role of the immune system and potential for immunotherapy. *Journal of*
602 *Thoracic Oncology, 10*(7), 974-984. doi:10.1097/JTO.0000000000000551
603 Chang, C. C., Chow, C. C., Tellier, L. C., Vattikuti, S., Purcell, S. M., & Lee, J. J. (2015).
604 Second-generation PLINK: rising to the challenge of larger and richer datasets.
605 *Gigascience, 4*, 7. doi:10.1186/s13742-015-0047-8
606 Chiba, T., Matsuzaka, Y., Warita, T., Sugoh, T., Miyashita, K., Tajima, A., . . . Kimura, M.
607 (2011). NFKBIL1 confers resistance to experimental autoimmune arthritis through the
608 regulation of dendritic cell functions. *Scandinavian Journal of Immunology, 73*(5), 478-
609 485. doi:10.1111/j.1365-3083.2011.02524.x
610 Chiba, T., Miyashita, K., Sugoh, T., Warita, T., Inoko, H., Kimura, M., & Sato, T. (2011).
611 IkappaBL, a novel member of the nuclear IkappaB family, inhibits inflammatory
612 cytokine expression. *FEBS Letters, 585*(22), 3577-3581.
613 doi:10.1016/j.febslet.2011.10.024
614 Davydov, E. V., Goode, D. L., Sirota, M., Cooper, G. M., Sidow, A., & Batzoglou, S. (2010).
615 Identifying a high fraction of the human genome to be under selective constraint using
616 GERP++. *PLoS Comput Biol, 6*(12), e1001025. doi:10.1371/journal.pcbi.1001025
617 Dolcet, X., Llobet, D., Pallares, J., & Matias-Guiu, X. (2005). NF-kB in development and
618 progression of human cancer. *Virchows Arch, 446*(5), 475-482. doi:10.1007/s00428-005-
619 1264-9
620 Dretzke, J., Edlin, R., Round, J., Connock, M., Hulme, C., Czeczot, J., . . . Meads, C. (2011). A
621 systematic review and economic evaluation of the use of tumour necrosis factor-alpha
622 (TNF-α) inhibitors, adalimumab and infliximab, for Crohn's disease. *Health Technology*
623 *Assessment (Winchester, England), 15*(6), 1. doi:10.3310/hta15060
624 Edwards, S. L., Beesley, J., French, J. D., & Dunning, A. M. (2013). Beyond GWASs:
625 illuminating the dark road from association to function. *American Journal of Human*
626 *Genetics, 93*(5), 779-797. doi:10.1016/j.ajhg.2013.10.012
627 ENCODE Project Consortium. (2012). An integrated encyclopedia of DNA elements in the
628 human genome. *Nature, 489*(7414), 57-74. doi:10.1038/nature11247

629 Ferreiro-Iglesias, A., Lesseur, C., McKay, J., Hung, R. J., Han, Y., Zong, X., . . . Li, Y. (2018).
630 Fine mapping of MHC region in lung cancer highlights independent susceptibility loci by
631 ethnicity. *Nature Communications, 9*(1), 1-12. doi:10.1038/s41467-018-05890-2
632 Fishilevich, S., Nudel, R., Rappaport, N., Hadar, R., Plaschkes, I., Iny Stein, T., . . . Cohen, D.
633 (2017). GeneHancer: genome-wide integration of enhancers and target genes in
634 GeneCards. *Database (Oxford), 2017*. doi:10.1093/database/bax028
635 Freedman, M. L., Monteiro, A. N., Gayther, S. A., Coetzee, G. A., Risch, A., Plass, C., . . . Mills,
636 I. G. (2011). Principles for the post-GWAS functional characterization of cancer risk loci.
637 *Nature Genetics, 43*(6), 513-518. doi:10.1038/ng.840
638 Gandhi, L., Rodríguez-Abreu, D., Gadgeel, S., Esteban, E., Felip, E., De Angelis, F., . . . Powell,
639 S. F. (2018). Pembrolizumab plus chemotherapy in metastatic non–small-cell lung
640 cancer. *New England Journal of Medicine, 378*(22), 2078-2092.
641 doi:10.1056/NEJMoa1801005
642 GTEx Consortium, Lonsdale, J., Thomas, J., Salvatore, M., Phillips, R., Lo, E., . . . Young, N.
643 (2013). The genotype-tissue expression (GTEx) project. *Nature Genetics, 45*(6), 580.
644 Hacker, H., & Karin, M. (2006). Regulation and function of IKK and IKK-related kinases. *Sci*
645 *STKE, 2006*(357), re13. doi:10.1126/stke.3572006re13
646 Hayden, M. S., & Ghosh, S. (2012). NF-kappaB, the first quarter-century: remarkable progress
647 and outstanding questions. *Genes & Development, 26*(3), 203-234.
648 doi:10.1101/gad.183434.111
649 Hoesel, B., & Schmid, J. A. (2013). The complexity of NF-κB signaling in inflammation and
650 cancer. *Molecular Cancer, 12*(1), 86. doi:10.1186/1476-4598-12-86
651 Hu, M.-M., & Shu, H.-B. (2017). Multifaceted roles of TRIM38 in innate immune and
652 inflammatory responses. *Cellular & Molecular Immunology, 14*(4), 331-338.
653 doi:10.1038/cmi.2016.66
654 Huang, Y. F., Gulko, B., & Siepel, A. (2017). Fast, scalable prediction of deleterious noncoding
655 variants from functional and population genomic data. *Nature Genetics, 49*(4), 618-624.
656 doi:10.1038/ng.3810
657 Ionita-Laza, I., McCallum, K., Xu, B., & Buxbaum, J. D. (2016). A spectral approach integrating
658 functional genomic annotations for coding and noncoding variants. *Nature Genetics,*
659 *48*(2), 214-220. doi:10.1038/ng.3477
660 Jia, X., Han, B., Onengut-Gumuscu, S., Chen, W. M., Concannon, P. J., Rich, S. S., . . . de
661 Bakker, P. I. (2013). Imputing amino acid polymorphisms in human leukocyte antigens.
662 *PLoS One, 8*(6), e64683. doi:10.1371/journal.pone.0064683
663 Karczewski, K. J., & Snyder, M. P. (2018). Integrative omics for health and disease. *Nature*
664 *Reviews: Genetics, 19*(5), 299-310. doi:10.1038/nrg.2018.4
665 Karimi, M., Goldie, L. C., Cruickshank, M. N., Moses, E. K., & Abraham, L. J. (2009). A critical
666 assessment of the factors affecting reporter gene assays for promoter SNP function: a
667 reassessment of− 308 TNF polymorphism function using a novel integrated reporter
668 system. *European Journal of Human Genetics, 17*(11), 1454-1462.
669 doi:10.1038/ejhg.2009.80
670 Karin, M., & Greten, F. R. (2005). NF-kappaB: linking inflammation and immunity to cancer
671 development and progression. *Nature Reviews: Immunology, 5*(10), 749-759.
672 doi:10.1038/nri1703

673 Kircher, M., Witten, D. M., Jain, P., O'Roak, B. J., Cooper, G. M., & Shendure, J. (2014). A
674 general framework for estimating the relative pathogenicity of human genetic variants.
675 *Nature Genetics, 46*(3), 310-315. doi:10.1038/ng.2892
676 Landrum, M. J., Lee, J. M., Riley, G. R., Jang, W., Rubinstein, W. S., Church, D. M., & Maglott,
677 D. R. (2014). ClinVar: public archive of relationships among sequence variation and
678 human phenotype. *Nucleic Acids Research, 42*(Database issue), D980-985.
679 doi:10.1093/nar/gkt1113
680 Lawrence, T. (2009). The nuclear factor NF-κB pathway in inflammation. *Cold Spring Harbor*
681 *Perspectives in Biology, 1*(6), a001651. doi:10.1101/cshperspect.a001651
682 Li, X., Yung, G., Zhou, H., Sun, R., Li, Z., Liu, Y., Ionita-Laza, I., Lin, X. (2020). A multi-
683 dimensional integrative scoring framework for predicting functional regions in the human
684 genome. *Harvard University Department of Biostatistics Technical Report*.
685 Liu, X., Wu, C., Li, C., & Boerwinkle, E. (2016). dbNSFP v3. 0: A one-stop database of
686 functional predictions and annotations for human nonsynonymous and splice-site SNVs.
687 *Human Mutation, 37*(3), 235-241.
688 McKay, J. D., Hung, R. J., Han, Y., Zong, X., Carreras-Torres, R., Christiani, D. C., . . . Amos,
689 C. I. (2017). Large-scale association analysis identifies new lung cancer susceptibility
690 loci and heterogeneity in genetic susceptibility across histological subtypes. *Nature*
691 *Genetics, 49*(7), 1126-1132. doi:10.1038/ng.3892
692 Mira, J.-P., Cariou, A., Grall, F., Delclaux, C., Losser, M.-R., Heshmati, F., . . . Riché, F. (1999).
693 Association of TNF2, a TNF-α promoter polymorphism, with septic shock susceptibility
694 and mortality: a multicenter study. *Journal of the American Medical Association, 282*(6),
695 561-568. doi:10.1001/jama.282.6.561
696 Ng, P. C., & Henikoff, S. (2003). SIFT: Predicting amino acid changes that affect protein
697 function. *Nucleic Acids Research, 31*(13), 3812-3814. doi:10.1093/nar/gkg509
698 Okamoto, K., Makino, S., Yoshikawa, Y., Takaki, A., Nagatsuka, Y., Ota, M., . . . Inoko, H.
699 (2003). Identification of I kappa BL as the second major histocompatibility complex-
700 linked susceptibility locus for rheumatoid arthritis. *American Journal of Human Genetics,*
701 *72*(2), 303-312. doi:10.1086/346067
702 Palucka, K., & Banchereau, J. (2012). Cancer immunotherapy via dendritic cells. *Nature*
703 *Reviews Cancer, 12*(4), 265-277. doi:10.1038/nrc3258
704 Pikarsky, E., Porat, R. M., Stein, I., Abramovitch, R., Amit, S., Kasem, S., . . . Ben-Neriah, Y.
705 (2004). NF-κB functions as a tumour promoter in inflammation-associated cancer.
706 *Nature, 431*(7007), 461-466. doi:10.1038/nature02924
707 Pollard, K. S., Hubisz, M. J., Rosenbloom, K. R., & Siepel, A. (2010). Detection of nonneutral
708 substitution rates on mammalian phylogenies. *Genome Research, 20*(1), 110-121.
709 doi:10.1101/gr.097857.109
710 Reva, B., Antipin, Y., & Sander, C. (2011). Predicting the functional impact of protein
711 mutations: application to cancer genomics. *Nucleic Acids Research, 39*(17), e118.
712 doi:10.1093/nar/gkr407
713 Rich, S. S., & Concannon, P. (2015). Role of Type 1 Diabetes-Associated SNPs on
714 Autoantibody Positivity in the Type 1 Diabetes Genetics Consortium: Overview.
715 *Diabetes Care, 38 Suppl 2*, S1-3. doi:10.2337/dcs15-2001
716 Ridker, P. M., Everett, B. M., Thuren, T., MacFadyen, J. G., Chang, W. H., Ballantyne, C., . . .
717 Anker, S. D. (2017). Antiinflammatory therapy with canakinumab for atherosclerotic

disease. *New England Journal of Medicine, 377*(12), 1119-1131. doi:10.1056/NEJMoa1707914

Ridker, P. M., MacFadyen, J. G., Thuren, T., Everett, B. M., Libby, P., & Glynn, R. J. (2017). Effect of interleukin-1beta inhibition with canakinumab on incident lung cancer in patients with atherosclerosis: exploratory results from a randomised, double-blind, placebo-controlled trial. *Lancet, 390*(10105), 1833-1842. doi:10.1016/s0140-6736(17)32247-x

Rogers, M. F., Shihab, H. A., Mort, M., Cooper, D. N., Gaunt, T. R., & Campbell, C. (2018). FATHMM-XF: accurate prediction of pathogenic point mutations via extended features. *Bioinformatics, 34*(3), 511-513. doi:10.1093/bioinformatics/btx536

Sammel, M. D., Ryan, L. M., & Legler, J. M. (1997). Latent variable models for mixed discrete and continuous outcomes. *Journal of the Royal Statistical Society: Series B (Statistical Methodology), 59*(3), 667-678.

Siepel, A., Bejerano, G., Pedersen, J. S., Hinrichs, A. S., Hou, M., Rosenbloom, K., . . . Haussler, D. (2005). Evolutionarily conserved elements in vertebrate, insect, worm, and yeast genomes. *Genome Research, 15*(8), 1034-1050. doi:10.1101/gr.3715005

Spitz, M. R., Gorlov, I. P., Amos, C. I., Dong, Q., Chen, W., Etzel, C. J., . . . Zhang, D. (2011). Variants in inflammation genes are implicated in risk of lung cancer in never smokers exposed to second-hand smoke. *Cancer Discovery, 1*(5), 420-429. doi:10.1158/2159-8290.CD-11-0080

Sun, R., & Lin, X. (2019). Genetic Variant Set-Based Tests Using the Generalized Berk–Jones Statistic With Application to a Genome-Wide Association Study of Breast Cancer. *Journal of the American Statistical Association, (ePub ahead of print)*, 1-13.

Takahashi, H., Ogata, H., Nishigaki, R., Broide, D. H., & Karin, M. (2010). Tobacco smoke promotes lung tumorigenesis by triggering IKKβ-and JNK1-dependent inflammation. *Cancer Cell, 17*(1), 89-97. doi:10.1016/j.ccr.2009.12.008

Tam, V., Patel, N., Turcotte, M., Bosse, Y., Pare, G., & Meyre, D. (2019). Benefits and limitations of genome-wide association studies. *Nature Reviews: Genetics, 20*(8), 467-484. doi:10.1038/s41576-019-0127-1

Taniguchi, K., & Karin, M. (2018). NF-kappaB, inflammation, immunity and cancer: coming of age. *Nature Reviews: Immunology, 18*(5), 309-324. doi:10.1038/nri.2017.142

Timofeeva, M. N., Hung, R. J., Rafnar, T., Christiani, D. C., Field, J. K., Bickeboller, H., . . . Landi, M. T. (2012). Influence of common genetic variation on lung cancer risk: meta-analysis of 14 900 cases and 29 485 controls. *Human Molecular Genetics, 21*(22), 4980-4995. doi:10.1093/hmg/dds334

Van Schouwenburg, P. A., Rispens, T., & Wolbink, G. J. (2013). Immunogenicity of anti-TNF biologic therapies for rheumatoid arthritis. *Nature Reviews Rheumatology, 9*(3), 164. doi:10.1038/nrrheum.2013.4

Visscher, P. M., Wray, N. R., Zhang, Q., Sklar, P., McCarthy, M. I., Brown, M. A., & Yang, J. (2017). 10 Years of GWAS Discovery: Biology, Function, and Translation. *American Journal of Human Genetics, 101*(1), 5-22. doi:10.1016/j.ajhg.2017.06.005

Walser, T., Cui, X., Yanagawa, J., Lee, J. M., Heinrich, E., Lee, G., . . . Dubinett, S. M. (2008). Smoking and lung cancer: the role of inflammation. *Proceedings of the American Thoracic Society, 5*(8), 811-815. doi:10.1513/pats.200809-100TH

Wang, Y., Wei, Y., Gaborieau, V., Shi, J., Han, Y., Timofeeva, M. N., . . . Houlston, R. S. (2015). Deciphering associations for lung cancer risk through imputation and analysis of

12,316 cases and 16,831 controls. *Eur J Hum Genet, 23*(12), 1723-1728. doi:10.1038/ejhg.2015.48

Wu, M. C., Lee, S., Cai, T., Li, Y., Boehnke, M., & Lin, X. (2011). Rare-variant association testing for sequencing data with the sequence kernel association test. *American Journal of Human Genetics, 89*(1), 82-93. doi:10.1016/j.ajhg.2011.05.029

Yung, G. Y. H. (2016). *Statistical methods for analyzing genetic sequencing association studies.* (PhD thesis). Harvard University, Harvard University. Retrieved from https://dash.harvard.edu/bitstream/handle/1/33493313/YUNG-DISSERTATION-2016.pdf?sequence=4&isAllowed=y

Zhang, Q., Lenardo, M. J., & Baltimore, D. (2017). 30 years of NF-kappaB: a blossoming of relevance to human pathobiology. *Cell, 168*(1-2), 37-57. doi:10.1016/j.cell.2016.12.012

Figure Captions

Figure 1. Gene-level Manhattan plots for association with lung cancer and SNP-level Manhattan plots marked with MACIE predictions. a, Gene-level Manhattan plot for lung squamous cell carcinoma. Each point represents one gene. All genes passing the Bonferroni-corrected threshold are colored black (even chromosomes) or red (odd chromosomes), with non-significant genes shown in grey. Labeled numbers note count of significant genes on each chromosome (see Supplementary Table S1 for list of all significant genes). The majority of significant SCC genes fall on chromosome 6. b-c, Gene-level Manhattan plot comparing significant squamous cell carcinoma genes against significant genes in (b) adenocarcinoma and (c) small cell carcinoma. Color corresponds to whether the gene is significant in just one disease or both. Only genes passing the Bonferroni-corrected significance threshold are displayed. d-e, SNP-level Manhattan plot for association with lung cancer where the points are additionally colored according to the MACIE prediction of inclusion in the (d) regulatory class and (e) conserved class. Labeled numbers note count of significant genes on top six chromosomes with most SNPs passing the marginal association threshold (see Materials and Methods) and possessing a MACIE regulatory prediction greater than 0.9 as well as top three chromosomes with most SNPs passing the marginal association threshold and possessing a MACIE conserved prediction greater than 0.9.

Figure 2. Highly-weighted annotation scores used to calculate MACIE probability of regulatory class in noncoding SNPs. a-f, Highly-weighted (see Supplementary Figure S1 for weights) regulatory annotation scores for SNPs associated with the inflammatory and immune responses, including (a) logarithm of peak H3K27Ac signal, (b) logarithm of peak H3K4Me1 signal, (c) peak RNA polymerase II signal, (d) logarithm of distance to closest transcription start site, (e)

799 logarithm of number of ChIP transcription factor binding site peaks across all cell types and
800 tissues, and (f) peak DNase I signal, all in ENCODE data. Dashed black line denotes an
801 empirical cumulative distribution function for the measure on the x-axis, i.e. the *(x,y)* position of
802 a point on the line illustrates that a variant scoring *x* on the given annotation has a value that is
803 greater than *y* percent (where *y* is measured according the secondary y-axis on the right) of all
804 variants passing the threshold for marginal association (see Materials and Methods) with SCC
805 (SNPs not discussed are shaded in gray). If a line drawn straight up from the x-axis through a
806 SNP intersects the black line at a value near 1, then that SNP possesses an annotation value
807 greater than most other SNPs demonstrating evidence of association with SCC. The x-axis shows
808 at least the second through ninety-eighth percentile for all annotations. All SNPs mentioned in
809 main text are plotted for completeness, including missense SNPs that are not evaluated using
810 regulatory annotations. Discussed gene is given in parentheses next to each SNP, although a
811 single SNP may be proximal to multiple genes. Not all SNPs possess a value for all annotations;
812 missing values are not plotted but are imputed as described in the original data sources (see
813 Materials and Methods). While SNPs predicted by MACIE as belonging to the regulatory class
814 do not always show the lowest p-values or most extreme scores, they possess an annotation
815 profile containing multiple notable measures that cumulatively contribute to a significant
816 MACIE prediction. SNPs with low regulatory predictions may demonstrate one or a few large
817 scores, but their overall annotation profile for this class consists of mostly unremarkable values.
818
819 **Figure 3.** Highly-weighted annotation scores used to calculate MACIE probability of
820 evolutionarily conserved class. a-f, Highly-weighted (see Supplementary Figure S1 for weights)
821 conservation annotation scores for SNPs associated with the immune and inflammatory

responses, including (a) GERP++ rejected substitution score, (b) phastCons primate score, (c), phastCons placental mammal score, (d) phyloP placental mammal score, (e) phastCons vertebrate score, and (f) phyloP vertebrate score, all plotted against marginal *P*-value for association with SCC. Dashed black line denotes an empirical cumulative distribution function for the measure on the x-axis. The x-axis shows at least the second through ninety-eighth percentile for all annotations. While SNPs predicted by MACIE as belonging to the conserved class do not always show the lowest p-values or most extreme scores, they possess an annotation profile containing multiple elevated measures that cumulatively contribute to a significant MACIE prediction.

Figure 4. MHC region MACIE scores as well as annotation scores and comprehensive variant scores for *HLA-DQA1* SNPs. a-b, MACIE regulatory (a) and conserved class (b) scores plotted against p-value for MHC SNPs. SNPs are colored according to their score for the complementary class, i.e. when the regulatory score is on the y-axis, the color corresponds to the conservation score, and when the conservation score is on the y-axis, the color corresponds to either the damaging protein function score (for nonsynonymous SNPs) or regulatory score (other SNPs). A very small p-value is not necessarily indicative of a high MACIE prediction. c-e, Individual SNP annotation scores and comprehensive ratings for significant SNPs in *HLA-DQA1* including (c) GERP++ rejected substitutions score, (d) phastCons vertebrate score, (e) CADD PHRED comprehensive score (higher indicates more deleterious), and (f) SIFT protein score (lower indicates more deleterious) plotted against *P* -value. We only show those SNPs passing the marginal association threshold with SCC (see Materials and Methods). Black dashed line shows the empirical distribution of these measures (using secondary y-axis on right side of plots) for all

845 SNPs across the genome meeting this significance threshold. Variants are colored as described in

846 EIGEN.

Appendix A: Fitting the MACIE Model

Suppose for a noncoding or synonymous SNP i and annotation class j ($j = 1,2$) we observe a set $\boldsymbol{y}_{ij} = \left(y_{ij1}, \ldots, y_{ijK_j}\right)$ of K_j different functional scores. Let $\boldsymbol{c}_i = (c_{i1}, c_{i2})$ denote the vector of unobserved latent functional binary class indicators, with c_{i1} a binary indicator for SNP i possessing regulatory function and c_{i2} a binary indicator for SNP i possessing evolutionarily conserved function. Then for $j = 1,2$ and $k = 1, \ldots, K_j$, the functional scores y_{ijk} are modeled using a GLMM that assumes their means $\mu_{ijk} = E(y_{ijk})$ are linear functions of the latent binary functional status indicators c_{ij} and the random effects b_{ijk}. Specifically, we assume

$$g_{jk}(\mu_{ijk}) = \beta_{0jk} + c_{ij}\beta_{1jk} + b_{ijk},$$

where g_{jk} is a canonical link function. We set $\boldsymbol{b}_{ij} = (b_{ij1}, \cdots, b_{ijk})' = \boldsymbol{\Lambda}_j \boldsymbol{f}_{ij}$ with $\boldsymbol{f}_{ij} \sim MVN(0, \boldsymbol{I})$ as a vector of length $P_j < L_j$ to reduce computational complexity, with $\boldsymbol{\Lambda}_j$ acting as factor loadings. This step is reasonable because many functional annotations likely attempt to measure the same few underlying variables, and we assume there are P_j of these variables.

The expectation maximization algorithm is used to fit the model. The algorithm, expectation steps, and maximization steps are similar to those previously described (Sammel et al., 1997) for latent variable models with mixed discrete and continuous outcomes. Expectations that cannot be evaluated in closed form are taken with Gauss-Hermite quadrature, and score equations that cannot be solved in closed form are updated with a one-step Fisher scoring procedure (Sammel et al., 1997). Given the fitted model parameters and a new SNP i' with corresponding annotation scores $\boldsymbol{y}_{i'1}$ and $\boldsymbol{y}_{i'2}$, the probability $p(\boldsymbol{c}_{i'} = \boldsymbol{z} | \boldsymbol{y}_{i'1}, \boldsymbol{y}_{i'2})$ is the MACIE score, where $\boldsymbol{z} = (z_1, z_2) \in \{0,1\} \times \{0,1\}$. The same model fitting procedure is used for nonsynonymous coding

869 SNPs, except we utilize a different set of annotations and training data (see Material and

870 Methods). Other sets of annotations may be used to probe different functional classes as well.

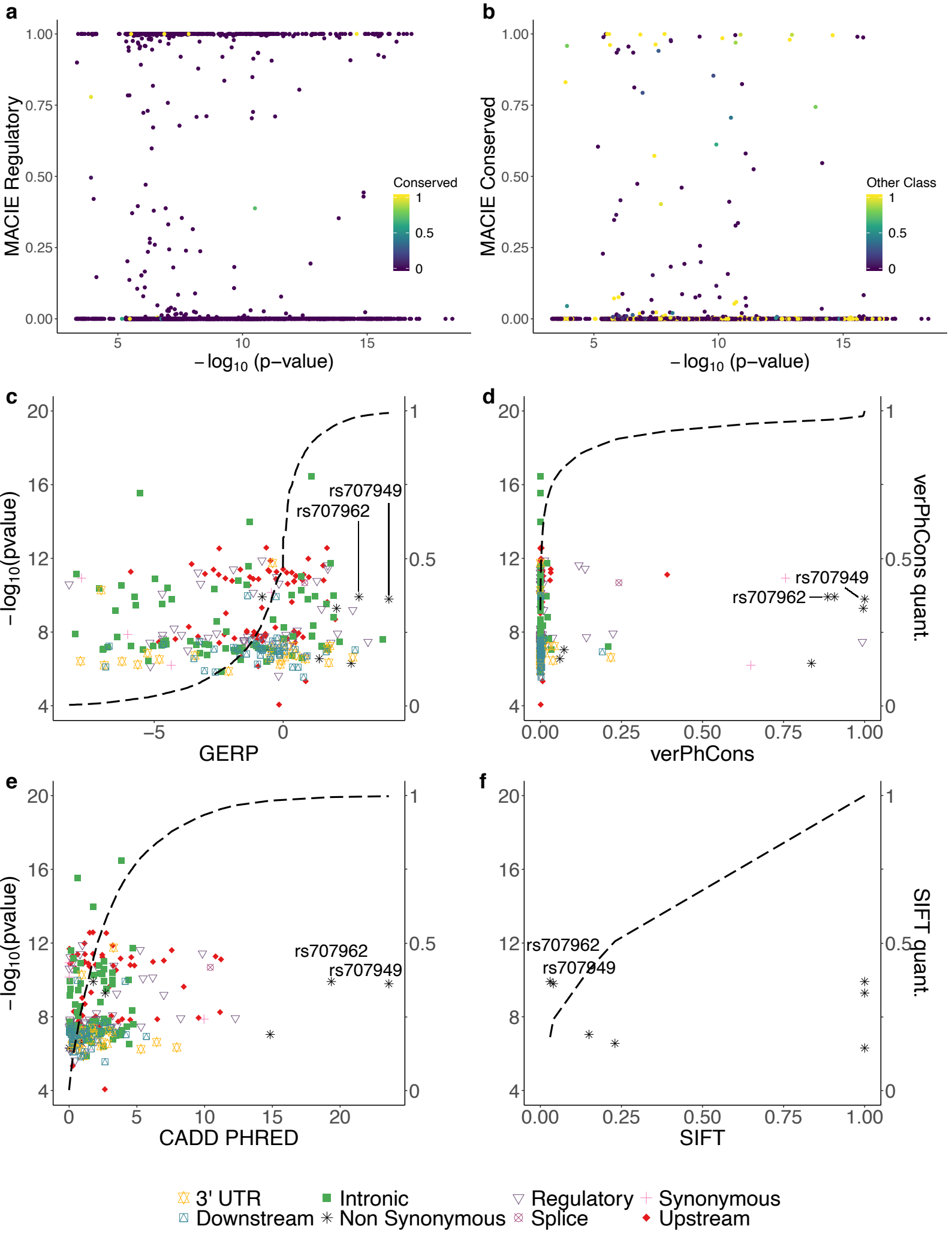
a
MACIE Regulatory
1.00
0.75
0.50
0.25
0.00
5
10
15
$-\log_{10}$ (p−value)
Conserved
1
0.5
0
b
MACIE Conserved
1.00
0.75
0.50
0.25
0.00
5
10
15
$-\log_{10}$ (p−value)
Other Class
1
0.5
0
c
$-\log_{10}$(pvalue)
20
16
12
8
4
1
0.5
0
−5
0
GERP
rs707949
rs707962
d
20
16
12
8
4
1
0.5
0
0.00
0.25
0.50
0.75
1.00
verPhCons
verPhCons quant.
rs707949
rs707962
e
$-\log_{10}$(pvalue)
20
16
12
8
4
1
0.5
0
0
5
10
15
20
CADD PHRED
rs707962
rs707949
f
20
16
12
8
4
1
0.5
0
0.00
0.25
0.50
0.75
1.00
SIFT
SIFT quant.
rs707962
rs707949
3' UTR
Downstream
Intronic
Non Synonymous
Regulatory
Splice
Synonymous
Upstream

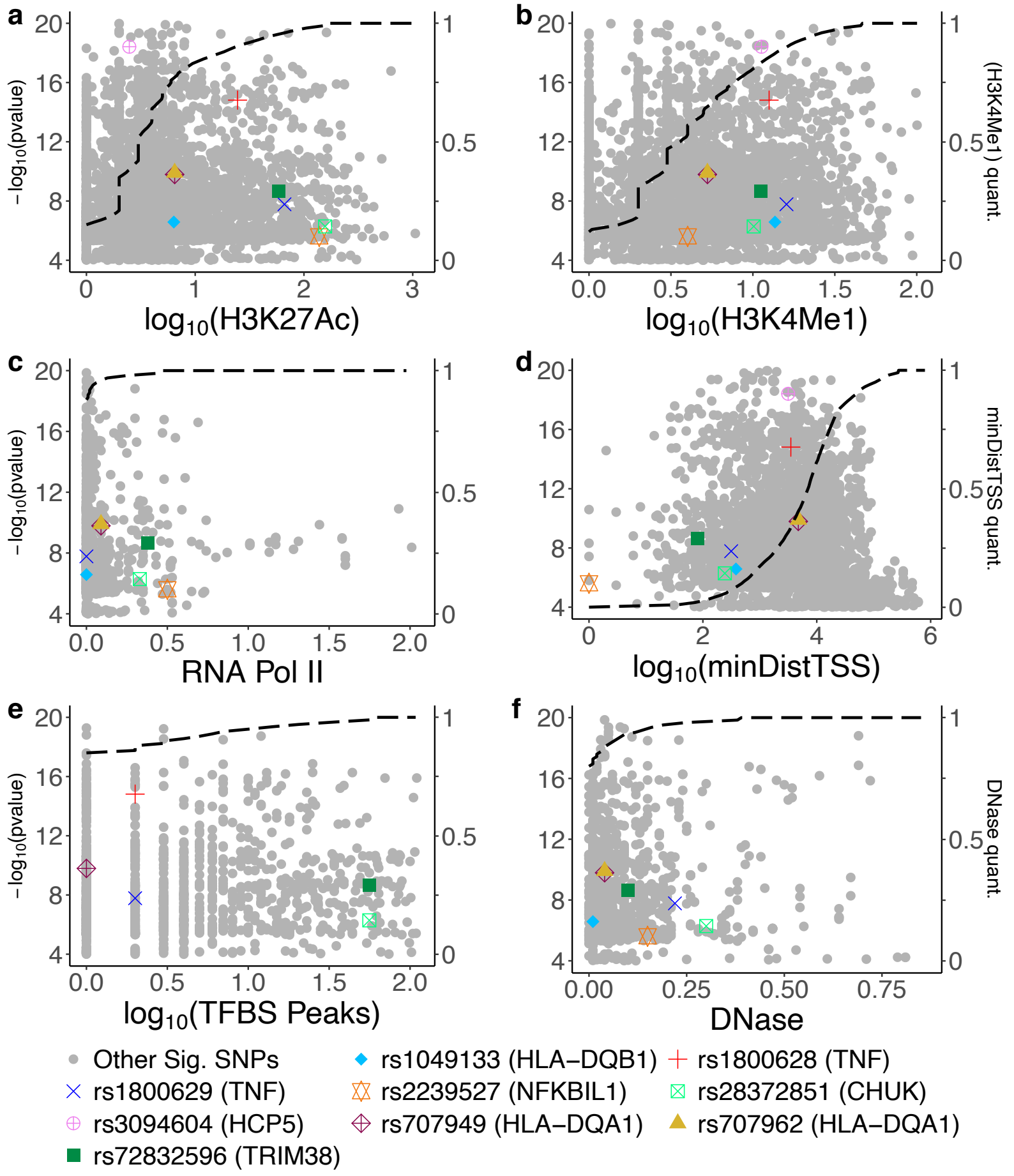
a
b
c
d
e
f
−log10(pvalue)
log10(H3K27Ac)
log10(H3K4Me1)
(H3K4Me1) quant.
RNA Pol II
log10(minDistTSS)
minDistTSS quant.
log10(TFBS Peaks)
DNase
DNase quant.
Other Sig. SNPs
rs1800629 (TNF)
rs3094604 (HCP5)
rs72832596 (TRIM38)
rs1049133 (HLA−DQB1)
rs2239527 (NFKBIL1)
rs707949 (HLA−DQA1)
rs1800628 (TNF)
rs28372851 (CHUK)
rs707962 (HLA−DQA1)

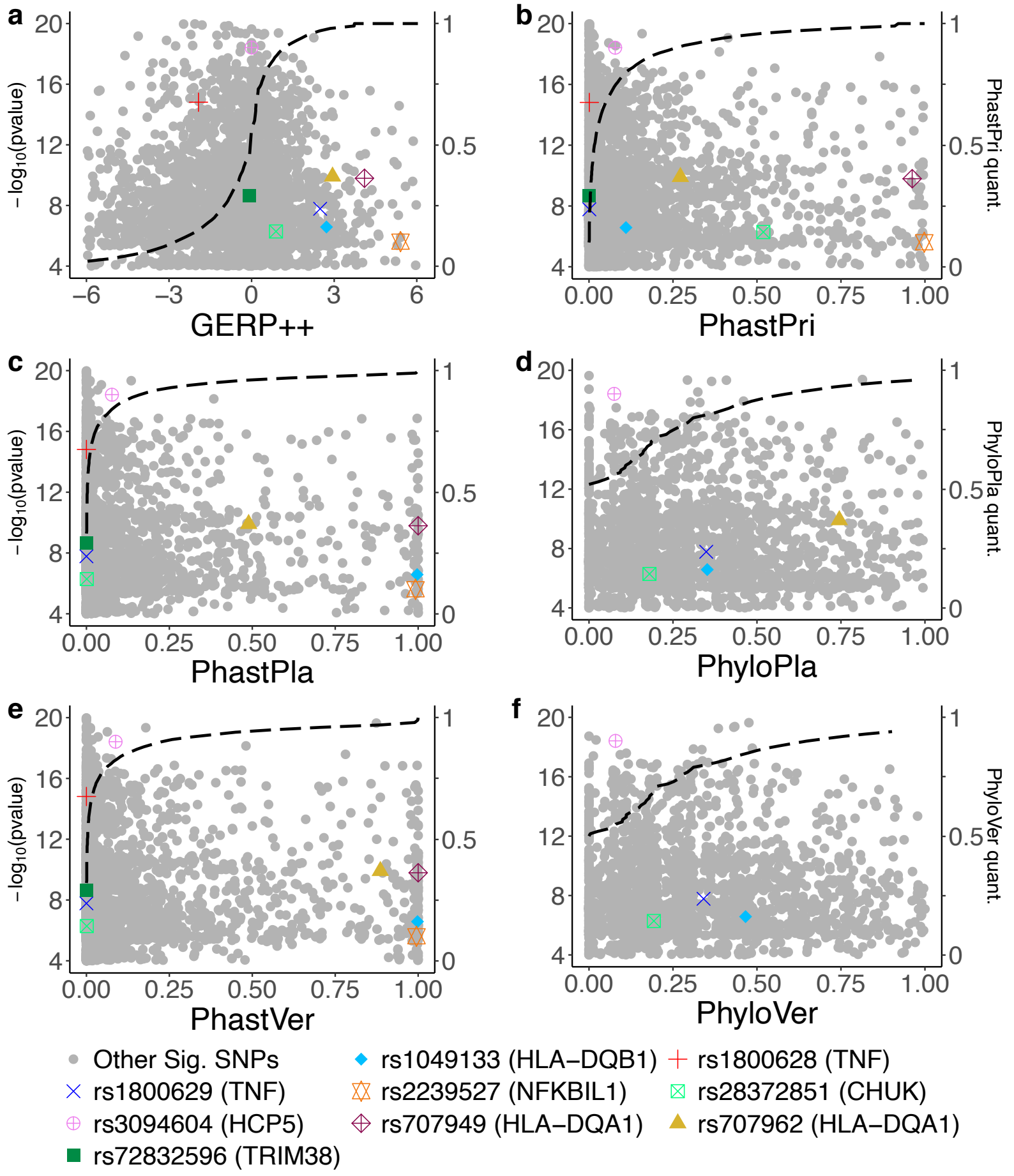
a
b
c
d
e
f
−log10(pvalue)
GERP++
PhastPri
PhastPri quant.
PhastPla
PhyloPla
PhyloPla quant.
PhastVer
PhyloVer
PhyloVer quant.
Other Sig. SNPs
rs1049133 (HLA−DQB1)
rs1800628 (TNF)
rs1800629 (TNF)
rs2239527 (NFKBIL1)
rs28372851 (CHUK)
rs3094604 (HCP5)
rs707949 (HLA−DQA1)
rs707962 (HLA−DQA1)
rs72832596 (TRIM38)